

A Cross-Layer Architecture of Wireless Sensor Networks for Target Tracking

Liang Song, *Member, IEEE*, and Dimitrios Hatzinakos, *Senior Member, IEEE*

Abstract—We propose the Low Energy Self-Organizing Protocol (LESOP) for target tracking in dense wireless sensor networks. A cross-layer design perspective is adopted in LESOP for high protocol efficiency, where direct interactions between the Application layer and the Medium Access Control (MAC) layer are exploited. Unlike the classical Open Systems Interconnect (OSI) paradigm of communication networks, the Transport and Network layers are excluded in LESOP to simplify the protocol stack. A lightweight yet efficient target localization algorithm is proposed and implemented, and a Quality of Service (QoS) knob is found to control the tradeoff between the tracking error and the network energy consumption. Furthermore, LESOP serves as the first example in demonstrating the migration from the OSI paradigm to the Embedded Wireless Interconnect (EWI) architecture platform, a two-layer efficient architecture proposed here for wireless sensor networks.

Index Terms—Application layer, embedded wireless interconnect, medium access control, open systems interconnect, target tracking, wireless sensor networks.

I. INTRODUCTION

ADVANCES in low-power electronics design have made it possible to develop highly integrated, yet low cost, micro-sensor nodes, with the capabilities of sensing, processing, and wireless communications. Once deployed, a network of thousands of these low-power micro-sensor nodes is expected to operate over years. Due to a large number of potential civil and military applications, a growing research interest has been directed in developing energy efficient self-organizing protocols for wireless sensor networks [1].

The unique nature of sensor networks, which are application specific and energy-resource limited, poses challenges in the network architecture design. Traditionally, wireless networks architecture is divided into hierarchical layers, based on the OSI architecture paradigm of computer networks [2]. However, in sensor networks, optimizations over the fundamental tradeoff between application specific QoS gain and energy cost suggest the breaking of OSI hierarchical layers, which has come to be known as “cross-layer design”.

In this paper, we consider the development of a dense wireless sensor network for target tracking applications. The Low Energy Self-Organizing Protocol (LESOP) is developed, which is based on the following considerations.

Manuscript received January 7, 2005; revised August 7, 2005 and December 7, 2005; approved by IEEE/ACM TRANSACTIONS ON NETWORKING Editor S. Das. This work was supported in part by Canadian Natural Sciences and Engineering Research Council (NSERC), and in part by the Bell University Labs at the University of Toronto.

The authors are with the Edward S. Rogers Sr. Department of Electrical and Computer Engineering, University of Toronto, Toronto, ON M5S 3G4, Canada (e-mail: songl@comm.utoronto.ca; dimitris@comm.utoronto.ca)

Digital Object Identifier 10.1109/TNET.2006.890084

A. Network QoS and Energy Consumption

The fundamental design tradeoff in wireless sensor networks is between application-specific QoS gain and energy consumption cost. For target tracking specifically, network QoS is decided by the tracking error, which is defined by the average target location estimation error. Under the assumption of uniform target distribution, the sensor networks lifetime under consideration is solely decided by the network energy consumption, which is the sum of the energy consumption on all sensor nodes. Thus, the fundamental design tradeoff can be more explicitly presented by the tradeoff between the tracking error and the network energy consumption.

B. Low-Complexity Signal Processing Requirement

The processing capability of micro-sensor nodes is usually highly limited due to limitations from energy resource and cost. This hampers the implementation of complicated signal processing algorithms on sensor nodes. Yet, a fully distributed, lightweight target localization/tracking algorithm is demanded.

C. Scalability

Since sensor networks are composed of thousands, or more, micro-sensor nodes, scalability in sensor network protocols is an important requirement. This suggests that protocol complexity should remain constant as node density increases. Moreover, it would be impossible for individual sensor nodes to obtain global information about the network. Also it is reasonable that, under dense deployment and dynamic environments, the knowledge of the network neighborhood may also be unavailable.

D. Event and Location Centric

Unlike traditional data communication networks, sensor networks are usually not address-centric. An individual sensor node generally does not have a globally unique ID in the network. For target tracking applications specifically, the data communication is event and location centric. Event centric suggests that network operation and wireless data exchange are triggered by events, i.e., the target detection in the interested region. Location centric suggests that the destination of wireless packets would be the nodes within a specific location region instead of one particular node. The two properties are compatible, in the sense that wireless communication takes place around the detected target location.

E. Separable Functionalities

The specific sensor network functionalities are the generation of track information and the delivery to a collector/sink. However, the two can be separately implemented. In the paper, we are only concerned with the track information generation,

which can be deemed as high-level event acquisition, as compared with raw data acquisition. The latter part, on the other hand, can be implemented by diverse schemes, such as geographical forwarding [3], [36] or Sensor Networks with Mobile Sinks (MSSN) [30], under different latency assumptions.

Under the above application-specific considerations, we develop the LESOP protocol by jointly designing the Application layer and the MAC layer. On the other hand, the Transport layer and the Network layer, which are important components of traditional communication network architectures, are removed. As detailed later, all the radio packets are simply broadcasted to the source node neighborhood wirelessly. In a sense, LESOP demonstrates the attributes of Connectionless Networking. Connectionless Networking [4], which has attracted research interest recently, mostly in military applications, advocates the consolidation of OSI layers headers and improving the energy efficiency by excluding initial link acquisition and shared routing information. More importantly, the cross-layer design in wireless sensor networks suggests the necessities of developing the new architecture for replacing the existing OSI paradigm [5], which should be visioned as revolutionary. Thus, we propose the Embedded Wireless Interconnect (EWI) as the potential universal architecture for sensor networks design. EWI is built on two layers, which are the System layer and the Wireless Link layer, respectively. ***The bottom Wireless Link layer supplies the library of wireless transmission modules to the upper System layer. The System layer judiciously decides the organization of the wireless links by exploiting the tradeoff between application-specific QoS gain and energy consumption expenditure.*** LESOP is shown as the first example demonstrating the paradigm migration from OSI to EWI in wireless sensor networks. We are able to identify explicitly the System layer and Wireless Link layer in LESOP, where the interaction interface between the two layers is also found concretely.

Next, under a target physical signal attenuation model, a low-complexity target localization algorithm is proposed and implemented in LESOP. A QoS knob ρ is employed in the Application layer, which decides the tradeoff between the target tracking error and the network energy consumption. The proposed protocol is fully scalable, since no global information or even the network neighborhood information is assumed at individual sensor nodes. Both analytical and simulation results show that LESOP achieves the desired application-specific properties.

In Section II, a literature survey is provided. Section III introduces the model assumptions. The LESOP protocol is described at high level in Section IV, and designed from a cross-layer perspective in Section V. Simulation results are provided in Section VI. The vision of the EWI platform is suggested in Section VII, where LESOP is shown as a design example. Discussions and conclusions are presented in Section VIII and Section IX, respectively.

II. RELATED WORK

Target localization/tracking has been considered as one of the major applications of wireless sensor networks. Most existing references have been focused on the Application layer and the Network layer.

The study on target source localization has a long history. A classification of existing approaches is based on a variety of different physical measurements, such as TOA/TDOA (Time of Arrival/Time Difference of Arrival) [6], AOA (Angle of Arrival) [7], and energy-based measurement [8]. In sensor networks, target localization can also be achieved by merely one bit detected/undetected information from sensor nodes [9]. A target localization protocol with energy-efficiency considerations was developed in [10] for sensor networks.

For target tracking sensor networks, research efforts have been focused on the handover of target tracking duty among leader nodes (or cluster heads). Zhao *et al.* proposed the IDSQ (Information Driven Sensor Querying) in [11] and [12], where a leader sensor node is intelligently selecting the best neighbor node to perform sensing and serve as the next leader. A cost function was employed by jointly considering the energy expenditure and information gain. Based on a similar idea, in [13], Wang *et al.* applied the Bayesian SMC (Sequential Monte Carlo) methods to the problem of optimal sensor selection and fusion in target tracking. These approaches require that individual sensor nodes process detailed information about all nodes in neighborhood, such as the location and residual energy level, which limits the protocol scalability. Moreover, the complexity of node selection algorithms might impose high constraints on sensor node processing capability.

Brooks *et al.* proposed location centric CSP (Collaborative Signal Processing) approaches for target tracking sensor networks in [14] and [15], where a selected region instead of an individual sensor node is activated. The location-centric proposal shares the same intuition as LESOP. However, since they are focused on upper layers (application and network) design, it is unclear how the CSP methods can be efficiently implemented in wireless sensor networks. Moreover, energy efficiency was not considered in the work of CSP. Zhang *et al.* proposed optimized tree reconfiguration for target tracking networks in [16], which is concentrated on the Network layer domain, and shaped by the tracking application requirements. Potential optimization in lower layers, however, was also not considered.

Related work also includes the coverage of sensor networks, where the goal is to find a small set of sensor nodes covering the interested surveillance region. In [17] and [18], deterministic protocols were proposed to achieve this goal, which are based on the distributed information exchange among sensor nodes. In this paper, however, we adopt a probabilistic approach under a detection time-delay parameter, which requires no inter-node information exchange. Compared with other probabilistic proposals [19], more explicit results are obtained in this paper.

Moreover, energy efficient MAC layer designs for general sensor networks can be found in PAMAS [20], S-MAC [21], T-MAC [22], and SIFT [23]. Compared with these works, in LESOP, we show how the application-specific requirements can shape the MAC design. It is also interesting to compare LESOP with LEACH [24] to show that different application requirements lead to totally different design considerations. LEACH is an energy-aware cluster head selection mechanism for environmental monitoring sensor networks, which assumes that sensor nodes continuously have data for transmission.

TABLE I
VARIABLES NOTATIONS AND PARAMETERS

Name	Description	Typical Value
t	Time variable	
\mathbf{A}_s	Set of nodes having detected the target	
\mathbf{A}_t	Set of nodes participating detection fusion	
$E_i(t)$	Sensing measurement of sensor node i at time t	
$E_{th,i}$	Detection threshold of sensor node i	
$E_s(t)$	Illuminated target signal power at t	
μ_i	Detection fusion coefficient locally calculated at node i	
H_1	Leader node one	
H_2	Leader node two	
$\mathbf{L}_T(t)$	Location coordinates vector of the target at time t	
$\hat{\mathbf{L}}_T(t)$	Estimated location coordinates of the target at time t	
\mathbf{L}_i	Location coordinates vector of the node i	
$\mathbf{L}[x], \mathbf{L}[y]$	x and y of the location coordinates vector \mathbf{L}	
N_s	Number of nodes having detected the target	
N_t	Number of nodes participating detection fusion	
$N_t^*(\rho)$	Optimal value of N_t decided by ρ	
P_{idle}	Average network power consumption per m^2 when target is not present	
P_{track}	Average network power consumption in target tracking	
T_{dec}	Target detection delay	
$T_d(\mu_i)$	MAC time delay of DEC_INFO packet, as a function of μ_i	
λ	Sensor node density	$0.1 \sim 1/m^2$
ρ	QoS knob coefficient	$0 \sim 0.5$
ES	Mean of $E_s(t)$	$12dBm$
σ_s	Standard deviation of $E_s(t)$	$1.2dBm$
σ_i^2	Sensing noise variance of sensor node i	$0dBm$
γ_i	Sensing gain of sensor node i	$0dB$
f_s	Sensing sampling frequency	$8kHz$
L_d	Length of DEC_INFO packet	$64 \times 8bit$
L_t	Length of TRACK_INFO packet	$128 \times 8bit$
L_a	Length of TRACK_ACK packet	$16 \times 8bit$
N	The number of samples in one sensing measurement	$20 \sim 100$
P_{FA}	Maximum false alarm probability	0.001
P_{sen}	Primary radio power consumption in sensing	$1mW$
P_t	Primary radio power consumption in transmitting	$15mW$
$P_{r/i}$	Primary radio power consumption in receiving and idling	$10mW$
$Range$	Radio transmission range	$15m$
R_{RF}	Primary radio bit rate	$20kbps$
T_{track}	Time interval between two consecutive target location estimations	$0.5s$
T_{sen}	Time interval between two consecutive sensing in IDLE state	$5s$
$T_{d,max}$	Maximum MAC time delay on DEC_INFO packet	$30ms$

III. MODEL ASSUMPTIONS

We assume single target tracking in the paper. Extensions to co-located multiple targets tracking is discussed in Section VIII-C. Under the assumption of uniform target distribution, load balancing in sensor networks is also achieved automatically by localized processing. For easy reference, Table I provides a list of parameters and variables notation used in the paper. Typical values of the parameters are also given.

A. Node Deploying Model

Consider a large number of sensor nodes randomly deployed over the surveillance region, where \mathbf{L}_i denotes the location coordinates of node i . As long as that the number of sensor nodes is large, the node distribution can be modelled as a homogeneous Poisson process [25] with the node density λ . That is, given an area of the size $|\mathbf{A}|$ in the field, the number of nodes in the area, $\mu(\mathbf{A})$, follows Poisson distribution with parameter $\lambda|\mathbf{A}|$, i.e.,

$$\text{Prob}(\mu(\mathbf{A}) = m) = e^{-\lambda|\mathbf{A}|} \cdot \frac{(\lambda \cdot |\mathbf{A}|)^m}{m!}, \quad m = 0, 1, \dots, \infty. \quad (1)$$

Note that the LESOP protocol does not necessarily depend on this model. The Poisson model is however useful in the analysis.

B. Sensor Detection Model

Sensors convert the target physical signal to an electric signal. The target is supposed to be moving in the surveillance region. Let $\mathbf{L}_T(t)$ denote the target location coordinates, where t is the time. Also, let $s(t)$ denote the physical signal of target. The sensed physical signal on sensor i , $r_i(t)$, is assumed to be modeled as

$$r_i(t) = \gamma_i \cdot \frac{s(t)}{\|\mathbf{L}_T(t) - \mathbf{L}_i\|} + \nu_i(t) \quad (2)$$

where γ_i denotes the sensor gain, and $\nu_i(t)$ denotes the additive noise component, which is assumed to be zero-mean white Gaussian with the variance σ_i^2 . Note that the propagation delay is omitted in (2), which can be approximated as long as the propagation distance is small.

At an individual sensor i , N samples of $r_i(t)$ are obtained with the sampling frequency f_s . The target signal power at the

sensor i , $E_i(t)$, is estimated by taking the average of all N samples. It can be written as

$$\begin{aligned} E_i(t) &= {}^{(a)} \frac{1}{N} \cdot \sum_{n=0}^{N-1} r_i^2 \left(t + \frac{n}{f_s} \right) \\ &= {}^{(b)} \frac{\gamma_i}{\|\mathbf{L}_T(t) - \mathbf{L}_i\|^2} \cdot \left\{ \frac{1}{N} \cdot \sum_{n=0}^{N-1} s^2 \left(t + \frac{n}{f_s} \right) \right\} \\ &\quad + \frac{1}{N} \cdot \sum_{n=0}^{N-1} \nu_i^2 \left(t + \frac{n}{f_s} \right) \\ &= {}^{(c)} \frac{\gamma_i}{\|\mathbf{L}_T(t) - \mathbf{L}_i\|^2} \cdot E_s(t) + \varepsilon_i(t) \end{aligned} \quad (3)$$

where (a) is obtained directly from (2), (b) is obtained by considering that the target is approximately stationary within the sampling time duration $\frac{N-1}{f_s}$, and (c) is obtained directly by the following definitions:

$$E_s(t) = \frac{1}{N} \cdot \sum_{n=0}^{N-1} s^2 \left(t + \frac{n}{f_s} \right) \quad (4)$$

and

$$\varepsilon_i(t) = \frac{1}{N} \cdot \sum_{n=0}^{N-1} \nu_i^2 \left(t + \frac{n}{f_s} \right). \quad (5)$$

$E_s(t)$ is the estimated original target signal power from the target at time t . It is simply modeled as a Gaussian random variable with the distribution

$$E_s(t) \sim N(ES, \sigma_s^2) \quad (6)$$

where ES is the mean, and σ_s^2 is the variance. Since $\nu_i(t)$ is white Gaussian, $\left\{ \nu_i^2 \left(t + \frac{n}{f_s} \right) \right\}$ are i.i.d. Chi-Square random variables [25] with the mean σ_i^2 and variance $2 \cdot \sigma_i^4$. If N is sufficiently large, by means of the central limit theorem, $\varepsilon_i(t)$ is approximated as a Gaussian random variable with mean σ_i^2 and variance $\frac{2 \cdot \sigma_i^4}{N}$, that is,

$$\varepsilon_i(t) \sim N \left(\sigma_i^2, \frac{2 \cdot \sigma_i^4}{N} \right). \quad (7)$$

Note that this measurement model was also employed in [8] for acoustic signal energy measurement. Practically, the Gaussian approximation on $\varepsilon_i(t)$ is achieved when $N > 20$. We further assume that the sensor node i has the knowledge of the parameters, σ_i^2 , γ_i , and N .

Assume that at each sensor i , the required maximum false alarm probability is P_{FA} . Due to (3) and the model of (7), the detection energy threshold of sensor i , $E_{th,i}$, can be obtained by [29]

$$E_{th,i} = \sigma_i^2 + Q^{-1}(P_{FA}) \cdot \sqrt{\frac{2 \cdot \sigma_i^4}{N}} \quad (8)$$

where

$$Q(x) = \frac{1}{\sqrt{\pi}} \cdot \int_{\frac{x}{\sqrt{2}}}^{\infty} e^{-t^2} dt.$$

Energy consumption in one sensing measurement is proportional to the number of samples per measurement, N . Let P_{sen} denote the sensor power consumption. The energy consumption in one measurement on one particular sensor is $P_{sen} \cdot (N/f_s)$.

C. Radio Model

LESOP sensor nodes are assumed to be equipped with two radios, a primary RF radio, and a secondary wakeup radio. Let *Range* denote the range of both radios. An important assumption is that the radio range is two times larger than the sensing range. Further discussion on the assumption appears in Section VIII-A.

The primary radio is used for routine wireless data packet transmission. Its transmitting power and rate are assumed to be fixed. Let R_{RF} denote the rate. We further assume that channel Error Control Coding (ECC) ensures the correct radio packet decoding in the case of noncollision. Primary radio can be working in three distinct modes, transmitting, receiving/idle, or sleeping. Let the node power consumption in transmitting and receiving/idle modes be denoted by P_t and $P_{r/i}$, respectively. The sleeping mode power consumption is practically 1000 times smaller than P_t and $P_{r/i}$, which is negligible.

The secondary wakeup radio [20], [26], [27] can only send or detect busy tones. Due to the simplified functionalities, wakeup radio can be designed of super low power consumption, which is around 1 μ W in active monitoring mode. This can be achieved either by special hardware design [26], or very low duty cycle [27]. The power consumption of wakeup radio is hence of the same level as the sleeping mode of primary radio, which is also negligible. Furthermore, in the following, we also assume that the wakeup radio has the capability of sending/detecting busy tones at two separate frequencies, which are denoted by \mathbf{B}_a and \mathbf{B}_b , respectively.

IV. HIGH LEVEL LESOP PROTOCOL DESCRIPTION

We propose a low-complexity processing algorithm for target tracking, which is based on the sensor measurements $\{E_i(t)\}$. At time t , a leader sensor node, H_1 forces all its neighboring nodes to perform sensing, by broadcasting a busy tone through the wakeup radio. Initially, H_1 is defined as the sensor node who first detects the target. Assume that N_s nodes (neighboring H_1) have detected the target at time t . Further, let \mathbf{A}_s denote the set of N_s nodes, with $|\mathbf{A}_s| = N_s$. There is

$$\mathbf{A}_s = \{i | E_i(t) > E_{th,i}, \|\mathbf{L}_i - \mathbf{L}_{H_1}\| < Range\}. \quad (9)$$

The ‘‘detection information’’ fusion is done at a newly elected leader node, which is denoted as $H_2 \in \mathbf{A}_s$. N_t out of N_s ($N_t \leq N_s$) nodes participate in the fusion, by sending the detection information to H_2 . Further, let \mathbf{A}_t ($\mathbf{A}_t \subset \mathbf{A}_s$) denote the set of N_t nodes, with $|\mathbf{A}_t| = N_t$. After obtaining the target location estimation $\hat{\mathbf{L}}_T(t)$, H_2 receives the ‘‘track information’’ from H_1 , which can include a profile of the target. Let T_{track} denote the time interval between two consecutive target location estimations. At time $t + T_{\text{track}}$, the node H_2 takes the role of H_1 , and the above procedure is repeated until the target disappears in the surveillance region.

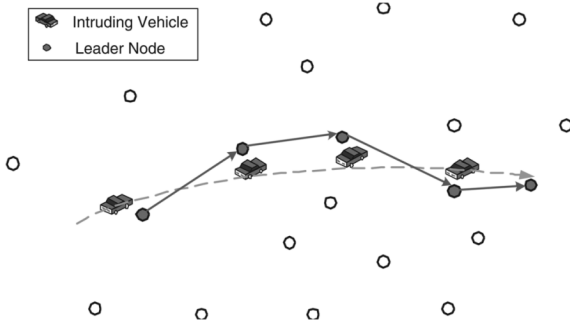


Fig. 1. LESOP illustration.

The above idea is illustrated in Fig. 1. Several problems need to be further clarified. First, what is the target location estimation mechanism based on detection information fusion, and what is the exchanged detection information? Second, how are the leader node H_2 and the set \mathbf{A}_t selected from \mathbf{A}_s in a self-organizing way? Third, if we have $H_2 \in \mathbf{A}_t$, $N_t - 1$ nodes need to transmit the detection information to H_2 . Thus, the network energy consumption in communication is proportional to $N_t - 1$. Nevertheless, it is also perceivable that the target localization error decreases with N_t . The question is how to exploit the tradeoff between the two by choosing an appropriate N_t . We will discuss the above three concerns in the following.

A. Target Location Estimation

We estimate the target location coordinates $\hat{\mathbf{L}}_{\mathbf{T}}(t)$ by means of optimal linear combining of $\{\mathbf{L}_i | i \in \mathbf{A}_t\}$

$$\hat{\mathbf{L}}_{\mathbf{T}}(t) = \sum_{i \in \mathbf{A}_t} w_i \cdot \mathbf{L}_i \quad (10)$$

where $\{w_i | i = 1 \dots N_t\}$, satisfying $\sum_{i \in \mathbf{A}_t} w_i = 1$, is the set of combining coefficients to be determined. $\{\mathbf{L}_i\}$ are known at the fusion center H_2 , being included in the detection information. $\mathbf{L}_{\mathbf{T}}(t)$ is treated as an unknown random vector.

For all $i \in \mathbf{A}_t$, we define δx_i and δy_i as

$$\delta x_i = \mathbf{L}_{\mathbf{T}}(t)[x] - \mathbf{L}_i[x] = D_i \cdot \cos \theta_i \quad (11)$$

and

$$\delta y_i = \mathbf{L}_{\mathbf{T}}(t)[y] - \mathbf{L}_i[y] = D_i \cdot \sin \theta_i \quad (12)$$

where

$$D_i = \|\mathbf{L}_{\mathbf{T}}(t) - \mathbf{L}_i\| \quad (13)$$

and θ_i is a uniformly distributed random variable in $[0, 2\pi)$, independent of D_i . Thus, the statistical expectation

$$E(\delta y_i) = E(\delta x_i) = E(D_i) \cdot E(\cos \theta_i) = 0 \quad (14)$$

and

$$\begin{aligned} E(\delta y_i^2) &= E(\delta x_i^2) \\ &= E(D_i^2) \cdot E(\cos^2 \theta_i) = \frac{1}{2} E(D_i^2). \end{aligned} \quad (15)$$

$E(D_i^2)$ is decided by

$$\begin{aligned} E(D_i^2) &= {}^{(a)} E(\|\mathbf{L}_{\mathbf{T}}(t) - \mathbf{L}_i\|^2) \\ &= {}^{(b)} E\left(\frac{E_s(t) \cdot \gamma_i}{E_i(t) - \varepsilon_i(t)}\right) \\ &= {}^{(c)} E_s(t) \cdot \gamma_i \cdot \sqrt{\frac{N}{4\pi\sigma_i^4}} \\ &\quad \cdot \int_{-\infty}^{+\infty} \frac{1}{E_i(t) - \sigma_i^2 - x} \cdot e^{-\frac{x^2 \cdot N}{4\sigma_i^4}} dx \end{aligned} \quad (16)$$

where (a) is by the definition in (13), (b) is obtained from the sensing model of (3), and (c) is by the normal distribution approximation of $\varepsilon_i(t)$, (7).

By means of optimal maximum ratio combining (MRC) theory [29], and (11), (12), (14), (15), we can write

$$w_i = \left(\frac{1}{E(D_i^2)}\right) / \left(\sum_{j \in \mathbf{A}_t} \frac{1}{E(D_j^2)}\right), \quad i \in \mathbf{A}_t \quad (17)$$

and by (10)

$$E(\|\mathbf{L}_{\mathbf{T}}(t) - \hat{\mathbf{L}}_{\mathbf{T}}(t)\|^2) = 1 / \left(\sum_{i \in \mathbf{A}_t} \frac{1}{E(D_i^2)}\right). \quad (18)$$

Since $E_s(t)$ is unknown at individual sensor nodes, $E(D_i^2)$ cannot be calculated directly to determine $\{w_i\}$. However, by defining

$$\begin{aligned} \mu_i &= \frac{E_s(t)}{E(D_i^2)} \\ &= \frac{1}{\gamma_i \cdot \sqrt{\frac{N}{4\pi\sigma_i^4}} \cdot \int_{-\infty}^{+\infty} \frac{1}{E_i(t) - \sigma_i^2 - x} \cdot e^{-\frac{x^2 \cdot N}{4\sigma_i^4}} dx} \\ & \quad i \in \mathbf{A}_s \end{aligned} \quad (19)$$

then (17) can be converted to

$$w_i = \frac{\mu_i}{\sum_{j \in \mathbf{A}_t} \mu_j}, \quad i \in \mathbf{A}_t. \quad (20)$$

μ_i can be calculated locally at individual sensor nodes, because only local information is needed in (19).

Thus, the ‘‘detection information’’ from individual sensor $i \in \mathbf{A}_t$ need only include μ_i and \mathbf{L}_i , which are sent to H_2 for information fusion. Furthermore, by means of (18), the estimation error variance can be written in the terms of $\{\mu_i\}$, as the following:

$$E(\|\mathbf{L}_{\mathbf{T}}(t) - \hat{\mathbf{L}}_{\mathbf{T}}(t)\|^2) = \frac{E_s(t)}{\sum_{i \in \mathbf{A}_t} \mu_i}. \quad (21)$$

B. Leader Node H_2 Election

By (21), given N_t , it is obvious that the N_t nodes in \mathbf{A}_t should be selected from \mathbf{A}_s as the set of nodes with the highest μ_i , that is,

$$\mu_i > \mu_j, \quad \forall i \in \mathbf{A}_t, \quad j \in \mathbf{A}_s - \mathbf{A}_t \quad (22)$$

in order to minimize the target localization error. Furthermore, by definition, the leader node H_2 is elected as the node with the highest μ_i , that is,

$$H_2 = \arg \max_{i \in \mathbf{A}_s} \mu_i. \quad (23)$$

This can be implemented by the MAC mechanism, described in Section V-B.

C. The QoS Knob ρ

$N_t - 1$ nodes in the set $\mathbf{A}_t - \{H_2\}$ need to transmit the detection information to the leader node H_2 . Both the communication energy consumption and the localization accuracy increase with N_t . Let us denote the improvement ratio on accuracy, when N_t is increased by 1, as $\chi(N_t)$. Then, according to (21), (22),

$$\begin{aligned} \chi(N_t) &= 1 - \frac{\sum_{i \in \mathbf{A}_t} \mu_i - \min\{\mu_j | j \in \mathbf{A}_t\}}{\sum_{i \in \mathbf{A}_t} \mu_i} \\ &= \frac{\min\{\mu_i | i \in \mathbf{A}_t\}}{\sum_{i \in \mathbf{A}_t} \mu_i}. \end{aligned} \quad (24)$$

Furthermore, based on (22), we find

$$\begin{aligned} \frac{\chi(N_t + 1)}{\chi(N_t)} &= \frac{\max\{\mu_i | i \in \mathbf{A}_t - \mathbf{A}_s\}}{\max\{\mu_i | i \in \mathbf{A}_t - \mathbf{A}_s\} + \sum_{i \in \mathbf{A}_t} \mu_i} \\ &\quad \cdot \frac{\sum_{i \in \mathbf{A}_t} \mu_i}{\min\{\mu_i | i \in \mathbf{A}_t\}} \\ &< \frac{\max\{\mu_i | i \in \mathbf{A}_t - \mathbf{A}_s\}}{\min\{\mu_i | i \in \mathbf{A}_t\}} \\ &\leq 1. \end{aligned} \quad (25)$$

Equation (25) suggests that $\chi(N_t)$ decreases monotonically with N_t . We propose to find the optimal value of N_t , $N_t^*(\rho)$, by a QoS knob coefficient ρ . ρ is conceptually defined as the minimum improvement ratio on accuracy at the cost of increasing N_t by one, which is,

$$N_t^*(\rho) = \min\{N_t | \chi(N_t) < \rho\}. \quad (26)$$

Obviously, $N_t^*(\rho)$ is a monotonically decreasing function of ρ . In other words, a higher ρ suggests that more emphasis is placed on network energy consumption, and the localization error is higher. Furthermore, the range of ρ should be $0 < \rho \leq 0.5$. The lower bound "0" is obvious. The upper bound "0.5" is due to the fact that $\chi(N_t) \leq 0.5$, for all $N_t > 1$. This is obtained straightforwardly from (22).

D. High Level Protocol Summary

Table II summarizes the high level LESOP protocol description, which is an iterative procedure for target tracking.

V. CROSS-LAYER LESOP PROTOCOL DESIGN

The system module architecture of LESOP node is shown in Fig. 2. The modules are named following the OSI tradition.

TABLE II
HIGH LEVEL LESOP PROTOCOL SUMMARIZATION

```

Given  $H_1$  at time  $t$ ;
Given  $\mathbf{A}_s$  by Eq.(9);
Obtain  $\{\mu_i\}$  locally on every node  $i \in \mathbf{A}_s$  by Eq.(19);
 $H_2$  is elected by Eq.(23);
if  $\mathbf{A}_s \neq \emptyset$ 
   $N_t = 1$ ;
   $\mathbf{A}_t = \{H_2\}$ ;
  While  $\chi(N_t) \geq \rho$  and  $\mathbf{A}_s - \mathbf{A}_t \neq \emptyset$  (Eq.(24))
     $N_t = N_t + 1$ ;
     $\mathbf{A}_t = \mathbf{A}_t \cup \{\arg \max_{i \in \mathbf{A}_s - \mathbf{A}_t} (\mu_i)\}$ ;
  end
   $N_t^*(\rho) = N_t$ ;
  Obtain  $\{w_i | i \in \mathbf{A}_t\}$  by Eq.(20);
  Obtain  $\hat{\mathbf{L}}_T(t)$  by Eq.(10);
   $H_1$  sending the old track information to  $H_2$ ;
   $H_2$  generating the new track information at time  $t$ ;
   $H_1 = H_2$  and repeat the procedure at  $t = t + T_{track}$ ;
else
  The target is assumed having disappeared.
end

```

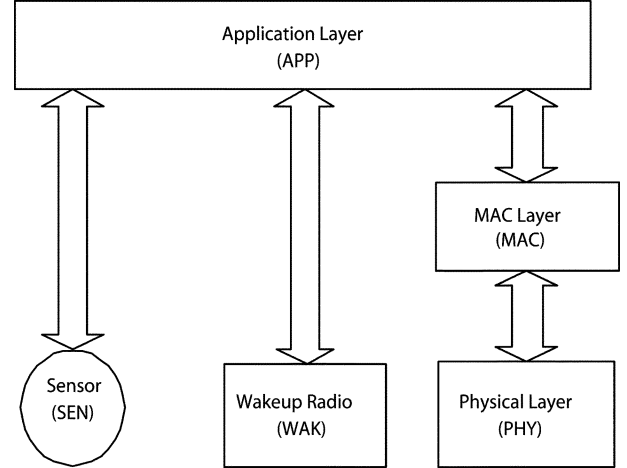


Fig. 2. LESOP modules.

However, as to be discussed later, in Section VII, the LESOP architecture virtually conforms to the proposed two-layer EWI platform.

Inter-module information exchanges are done by messages. On the other hand, inter-node communications are done by packets and busy tones. Packets go through the primary radio, while busy tones are sent by the secondary wakeup radio. We further define the set of inter-module messages, inter-node packets/tones, and module states for LESOP in Table III. For wireless communications specifically, the Transport and Network layer are omitted to simplify the protocol stack. All the radio packets have one source address, which is the location coordinates \mathbf{L}_i of the source sensor node. However, they do not have a destination address, and are wirelessly broadcasted to the source neighborhood.

A. Application Layer

The role of the Application layer is the overall control of the node functionalities. All the inter-node communications (packets or busy tones) start and end at the particular node Application layer. It can be in one of the following four states,

TABLE III
DEFINITIONS OF MESSAGES, PACKETS, BUSY TONES, AND MODULE STATES

Type	Name	Description
Message	SEN_POLL	APP → SEN: Activating Sensor
Message	SEN_MEASURE	SEN → APP: Reporting $E_i(t)$
Message	DEC_READY	MAC → APP: Indicating Ready to Send
Message	DEC_CANCEL	APP → MAC: Canceling Current DEC_INFO
Message	DEC_SET	APP → MAC: Confirming Current DEC_INFO
Message	RADIO_ACT	APP → PHY: Turning on Primary Radio
Message	RADIO_SLE	APP → PHY: Turning off Primary Radio
Packet	DEC_INFO	Detection Inform.; Including μ_i, L_i ; Length L_d
Packet	TRACK_INFO	Track Information; Length L_t
Packet	TRACK_ACK	Acknowledge of TRACK_INFO; Length L_a
Busy Tone	B_a	Busy Tone at Frequency a
Busy Tone	B_b	Busy Tone at Frequency b
State	IDLE	Application Layer State
State	WAIT	Application Layer State
State	HEADI	Application Layer State
State	HEADII	Application Layer State
State	TRANSMIT	Primary Radio Physical Layer State
State	RECEIVE/IDLE	Primary Radio Physical Layer State
State	SLEEP	Primary Radio Physical Layer State

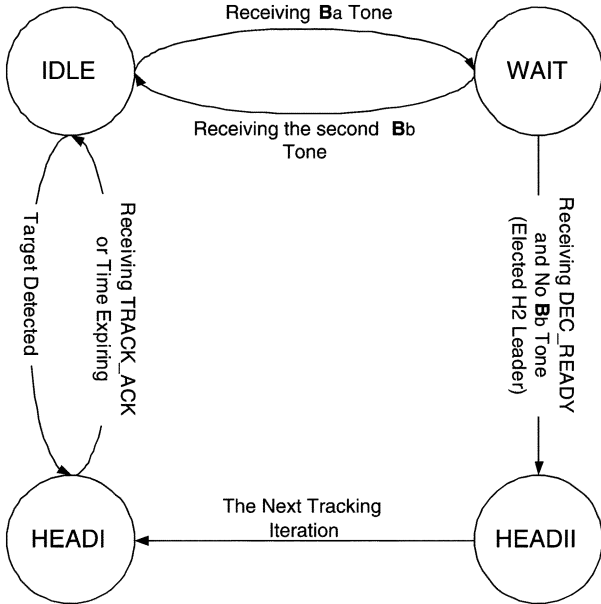


Fig. 3. Application layer states diagram.

IDLE, WAIT, HEADI, HEADII. The state transfer diagram is shown in Fig. 3.

1) *IDLE State*: In IDLE state, it is assumed that the target is undetected in the neighborhood region of the node. Note that initially all the deployed sensor nodes are in IDLE state. The Application layer periodically polls the sensor (sending SEN_POLL message) and read the sensing measurement $E_i(t)$ (retrieving SEN_MEASURE message). This time period, T_{sen} , indicates how fast the target can be detected after appearing in the surveillance region. More specifically, let the random variable T_{dec} denote the detection delay, which is the time difference between the time the target appears, and the first time that the target is detected. The expected value of T_{dec} , $E(T_{dec})$, can be shown upper bounded by (see Appendix I)

$$E(T_{dec}) \leq \frac{T_{sen}}{\lambda \cdot \delta p} \quad (27)$$

where

$$\delta p = \frac{\pi}{\sqrt{2\pi\sigma_s^2}} \cdot \int_{-\infty}^{+\infty} \int_{0^+}^{+\infty} Q\left(Q^{-1}(P_{FA}) - \frac{\min(\gamma_i) \cdot x}{y}\right) \cdot \sqrt{\frac{N}{2\max(\sigma_i^4)}} \cdot e^{-\frac{(x-ES)^2}{2\sigma_s^2}} dx dy. \quad (28)$$

Once the target is detected ($E_i(t) > E_{th,i}$), the Application layer sends through the wakeup radio the busy tone B_a , and transfers to HEADI state. B_a forces all the neighboring sensor nodes become active. On the other hand, if B_a arrives first, the Application layer sends SEN_POLL and transfers to WAIT state.

2) *Wait State*: In WAIT state, the Application layer first retrieves SEN_MEASURE message from the sensor. If the measurement $E_i(t) < E_{th,i}$, it simply returns to IDLE state at the end of the track interval T_{track} . Otherwise, if $E_i(t) > E_{th,i}$, μ_i is calculated locally by (19). μ_i is then included in the DEC_INFO packet and forwarded to the MAC layer.

The first B_b busy tone indicates that the leader node H_2 has been elected in the neighborhood. When the DEC_READY message is received from the MAC layer, the specific node becomes H_2 , if H_2 has not been elected. Correspondingly, the Application layer transfers to HEADII state, and sends DEC_CANCEL message to the MAC layer to cancel the current DEC_INFO packet. On the other hand, if it is known that H_2 has been elected upon receiving DEC_READY, the Application layer replies to the MAC layer with the confirmation DEC_SET message.

The second B_b busy tone indicates that the target location estimation procedure has ended. When it arrives, the Application layer sends DEC_CANCEL message to the MAC layer, and transfers to IDLE state.

3) *HEADI State*: In HEADI state, the node behaves as the H_1 node. The Application layer waits for the second B_b busy tone from the wakeup radio. Once the desired B_b arrives, it sends TRACK_INFO packet through the primary radio, and waits for the acknowledge, TRACK_ACK packet, from H_2 node. After the exchange, the Application layer goes to the IDLE state.

If the second \mathbf{B}_b does not arrive within the track interval limit T_{track} , the node decides that the target has disappeared or errors have occurred. Application layer transfers to IDLE state, and the track record is then forwarded to the sink by other mechanisms.

4) *HEADII State*: In HEADII state, the node behaves as the H_2 node. First, \mathbf{B}_b busy tone is broadcasted through the wakeup radio, which announces that H_2 has been elected. RADIO_ACT message is then sent to set the Physical layer in RECEIVE/IDLE state (turning on primary radio).

The Application layer receives DEC_INFO packets from the neighborhood in sequence. The detection information fusion process is then executed as described in Table II. Once the terminating condition (26) is met, or the track interval time limit T_{track} is reached, the target location is estimated by (10). The second \mathbf{B}_b is then broadcasted through the wakeup radio, indicating that the estimation procedure has finished.

After the broadcasting of the second \mathbf{B}_b , the Application layer waits for TRACK_INFO packet from H_1 , and responds with the acknowledge, TRACK_ACK packet. The Application layer then sends a RADIO_SLE message to set the Physical layer in SLEEP state (turning off primary radio). When the track interval time T_{track} is reached, \mathbf{B}_a is broadcasted through the wakeup radio, and the Application layer transfers to HEADI state.

B. MAC Layer

Upon receiving the forwarded DEC_INFO packet from the Application layer, the MAC layer calculates a time delay for the DEC_INFO packet. Intuitively, the delay is inversely proportional to the μ_i of the specific DEC_INFO packet. By $T_d(\mu_i)$ denoting the specific delay, we set

$$T_d(\mu_i) = \frac{A}{\mu_i} \quad (29)$$

where A is a preset constant, satisfying

$$A = \frac{T_{d,\max}}{\max_i \left\{ \gamma_i \sqrt{\frac{N}{4\pi\sigma_i^4}} \cdot \int_{-\infty}^{+\infty} \frac{1}{E_{th,i} - \sigma_i^2 - x} e^{-\frac{x^2 \cdot N}{4\sigma_i^4}} dx \right\}} \quad (30)$$

In (30), $T_{d,\max}$ is the maximum value of the delay under consideration. Due to (19), $T_{d,\max}$ is obtained only when μ_i reaches its minimum. The delay mechanism of $T_d(\mu_i)$ ensures that the node with highest μ_i would be elected as the leader node H_2 , by (23). It also ensures that the set of nodes, \mathbf{A}_t , are of the highest μ_i , as described in the rule of (22).

Specifically, the MAC layer waits until the expiration of the time delay $T_d(\mu_i)$ to perform radio carrier sensing. If the primary radio channel is busy, the MAC layer waits for another time delay, L_d/R_{RF} , which is the DEC_INFO packet transmission delay. When the radio channel is free, DEC_READY is sent to the Application layer. If the response is DEC_SET, the DEC_INFO packet is forwarded to Physical layer and broadcasted. Otherwise, if the Application layer response is DEC_CANCEL, the DEC_INFO packet is deleted in MAC.

TABLE IV
MAC LAYER PROCESSING OF DEC_INFO PACKET

Obtain DEC_INFO packet from Application layer; Calculate $T_d(\mu_i)$ by Eq.(29); Wait for the time duration $T_d(\mu_i)$; While (Radio Channel is Busy) Wait for the time duration $\frac{L_d}{R_{RF}}$; end Send DEC_READY to Application layer; If (get DEC_SET from Application layer) Forward DEC_INFO packet to Physical layer; else Purge DEC_INFO on MAC; end

This procedure is summarized in Table IV. Moreover, at any time when DEC_CANCEL message is received, the current DEC_INFO packet awaiting in the buffer is deleted.

Upon receiving TRACK_INFO or TRACK_ACK packets from the Application layer, the MAC performs radio carrier sensing, and waits until the radio channel is free. The TRACK_INFO or TRACK_ACK packets are then forwarded to the Physical layer and broadcasted. The MAC layer also forwards all the received packets from the Physical layer to the Application layer.

Note that a collision of DEC_INFO packets can occur when, for two nodes i and j , $|T_d(\mu_i) - T_d(\mu_j)| < (Range/3 \times 10^8)$. This is the maximum propagation delay of radio packets in air. Since *Range* is small in sensor networks, the collision probability is practically small. Moreover, the LESOP protocol is virtually robust to the collision, since H_2 can ignore the collision, and wait for the next successfully received DEC_INFO packet. Furthermore, we also assign the channel error control coding (ECC) functionality to the MAC layer. Note that traditionally, ECC is defined at Data Link layer, and MAC is a sub-layer of Data Link layer. This contradiction is virtually nonimportant here, and provides us with an efficient way of presentation.

C. Physical Layer, Wakeup Radio, and Sensor

The Physical layer of primary radio is responsible for broadcasting the radio packets to the node's neighborhood, which in our simplified model is a circular region with radius *Range*. It also supplements carrier sensing capability to MAC layer, and detects radio packets collision on primary radio. As described in the model of Section III-C, the Physical layer can be in one of the three states, TRANSMIT, RECEIVE/IDLE, and SLEEP, which correspond to the three modes of primary radio, transmitting, receiving/idle, and sleeping, respectively. When receiving the forwarded packets from the MAC layer, the Physical layer goes to TRANSMIT state, and returns to the previous state after transmission. The Application layer can configure the Physical layer in RECEIVE/IDLE or SLEEP states, by RADIO_ACT or RADIO_SLE messages, respectively.

The wakeup radio and the sensor modules are under control of the Application layer. Wakeup radio broadcasts the busy tone forwarded from the Application layer, and sends the detected busy tone to the Application layer. Only upon receiving SEN_POLL message from Application layer, the sensor module is activated, senses and replies the measurement $E_i(t)$ by SEN_MEASURE message.

D. Power Consumption Analysis

1) *Network Idle Power Consumption*: When the target is not present, we define the network idle power consumption P_{idle} as the average power consumption per square meter (W/m^2) in the surveillance region. Since the energy consumption in one sensing measurement is $P_{\text{sen}} \cdot (N/f_s)$ (Section III-B), the power consumption is $P_{\text{sen}} \cdot \frac{N}{f_s \cdot T_{\text{sen}}}$. Given the node density λ , P_{idle} is a constant:

$$P_{\text{idle}} = \lambda \cdot P_{\text{sen}} \cdot \frac{N}{f_s \cdot T_{\text{sen}}}. \quad (31)$$

In (31), the network idle power consumption P_{idle} is inversely proportional to the parameter T_{sen} . Moreover, in (29), the expected detection delay $E(T_{\text{dec}})$ is linearly proportional to T_{sen} . Hence, T_{sen} decides the tradeoff between the two.

2) *Tracking Power Consumption*: When the target is present in the surveillance region, we denote P_{track} as the network power consumption in tracking. Note that the energy consumption E_{h2} of the H_2 node, in one iteration of the process described in Table II, is

$$E_{h2} = (N_t^*(\rho) - 1) \cdot \frac{L_d}{R_{\text{RF}}} \cdot P_{r/i} + \left(\frac{L_t}{R_{\text{RF}}} + T_{d,\text{max}} \right) \cdot P_{r/i} + \frac{L_a}{R_{\text{RF}}} \cdot P_t. \quad (32)$$

Furthermore, the energy consumption E_{h1} of the H_1 node, in one iteration, is

$$E_{h1} = \frac{L_a}{R_{\text{RF}}} \cdot P_{r/i} + \frac{L_t}{R_{\text{RF}}} \cdot P_t. \quad (33)$$

The average of other energy consumption, E_{other} , includes energy consumption in sensing and transmitting DEC_INFO packets, which is

$$E_{\text{other}} = \pi \cdot \text{Range}^2 \cdot \lambda \cdot P_{\text{sen}} \cdot \frac{N}{f_s} + \frac{L_d}{R_{\text{RF}}} \cdot P_t \cdot (N_t^*(\rho) - 1). \quad (34)$$

Thus,

$$P_{\text{track}} = \frac{E_{h1} + E_{h2} + E_{\text{other}}}{T_{\text{track}}} = C + (N_t^*(\rho) - 1) \cdot \frac{L_d \cdot (P_t + P_{r/i})}{R_{\text{RF}} \cdot T_{\text{track}}} + \pi \cdot \text{Range}^2 \cdot \lambda \cdot \frac{P_{\text{sen}} \cdot N}{f_s \cdot T_{\text{track}}} \quad (35)$$

where C is a constant:

$$C = \frac{L_t + L_a}{R_{\text{RF}} \cdot T_{\text{track}}} \cdot (P_t + P_{r/i}) + \frac{T_{d,\text{max}} \cdot P_{r/i}}{T_{\text{track}}}. \quad (36)$$

By (35), the power consumption in target tracking, P_{track} , can be divided into three portions. The constant portion C is the power consumption in exchanging ‘‘track information’’ (TRACK_INFO and TRACK_ACK) between elected leader nodes, and the power consumption of H_2 during idle listening. The second portion is the power consumption in the wireless

communication of DEC_INFO packets, which is controlled by the QoS knob ρ . By (26), $N_t^*(\rho)$ decreases with ρ . Thus, a larger ρ reduces power consumption, but increases tracking error ((21)). The third portion in (35) is the power consumption during sensing, which increases linearly with the number of samples N . On the other hand, higher N results in higher $\{\mu_i\}$, by (19). And higher $\{\mu_i\}$ results in lower localization error, by (21).

VI. SIMULATION STUDIES

A. Comparisons in Target Localization

The high level comparisons of target localization algorithms are performed by simulations using Matlab. Let 80 sensor nodes be uniformly randomly distributed in a 20×20 m square region. The target position is also randomly generated in the square. The parameters values agree with the list in Table I. The simulation results are averaged over 20000 Monte Carlo runs.

We compare the target localization algorithm in LESOP with the optimal Maximum Likelihood (ML) localization. In contrary to the linear combining in (10) of LESOP, the ML method is a nonlinear procedure, and is optimal in the sense of maximum likelihood. The ML estimation of target location $\hat{\mathbf{L}}_{\text{TML}}(t)$, given $\{E_i(t), \mathbf{L}_i | i \in \mathbf{A}_t\}$, is

$$\hat{\mathbf{L}}_{\text{TML}}(t) = \arg_{\mathbf{L}_{\text{T}}(t)} \max_{\mathbf{L}_{\text{T}}(t), E_s(t)} \left\{ \prod_{i \in \mathbf{A}_t} \text{Prob}(E_i(t) | \mathbf{L}_i, \mathbf{L}_{\text{T}}(t)) \right\} \quad (37)$$

where the probability $\text{Prob}(E_i(t) | \mathbf{L}_i, \mathbf{L}_{\text{T}}(t))$ is given by

$$\text{Prob}(E_i(t) | \mathbf{L}_i, \mathbf{L}_{\text{T}}(t)) = \sqrt{\frac{N}{4\pi \cdot \sigma_i^4}} \cdot e^{-\frac{N \cdot \left(E_i(t) - \sigma_i^2 - \frac{E_s(t) \cdot \gamma_i}{\|\mathbf{L}_{\text{T}}(t) - \mathbf{L}_i\|^2} \right)^2}{4\sigma_i^4}} \quad (38)$$

based on the model of (3) and (7). From (37), we implement the ML algorithm as a three-dimensional exhaustive search in the solution space, $\mathbf{L}_{\text{T}}(t)[x]$, $\mathbf{L}_{\text{T}}(t)[y]$, and $E_s(t)$. Moreover, we fix $N_t = 3$ for the ML algorithm.

Another target localization scheme included in comparisons is the Centroid Point (CP) approach, which equally weights the N_t nodes with the highest μ_i in calculating the estimated target location [i.e., in (10)]. Let $\hat{\mathbf{L}}_{\text{TCP}}(t)$ denote the estimation. Again, we fix $N_t = 3$ for the CP approach.

Fig. 4 compares the target localization error of LESOP, Maximum Likelihood, and Centroid Point, when the number of sampling per measurement, N , varies. Generally, in all schemes, the localization error decreases, when N increases. This is because of that measurements are of higher accuracy with larger N . Moreover, Fig. 4 shows that the localization error increases when the QoS knob ρ decreases, which agrees with our former analysis. At the cost of much higher complexity, the ML method achieves lower localization error than LESOP, which is about 0.3–0.4 m in the simulation. Fig. 5 plots $N_t^*(\rho)$ as a function of ρ , for $N = 20, 40, 100$, respectively. $N_t^*(\rho)$ decreases with ρ , and is generally below 3 in the simulation, except for $\rho = 0.15$. Remember that we fix $N_t = 3$ in the ML and CP algorithm. The results in Fig. 5 also suggest that comparisons in Fig. 4 are fair,

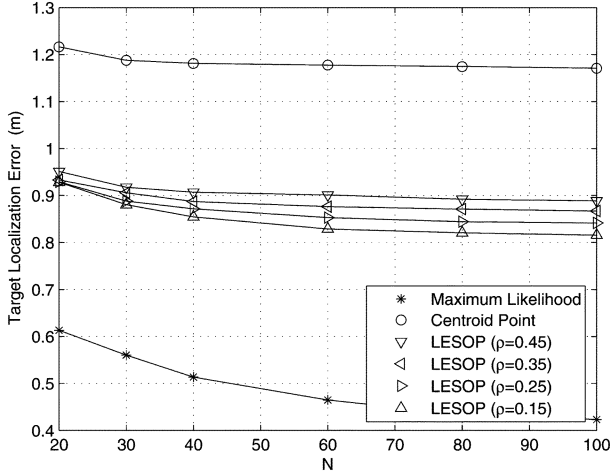
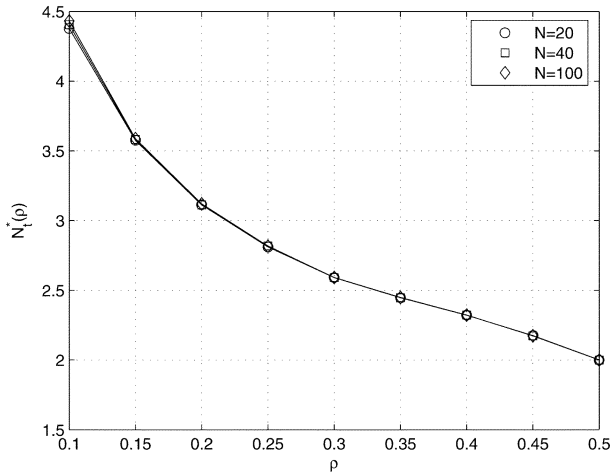


Fig. 4. Target localization error comparisons.

Fig. 5. $N_t^*(\rho)$ as a function of ρ .

because LESOP generally uses less information in the target location estimation.

B. Network Simulations

LESOP network protocol is simulated via the discrete event simulation system OMNet++ [28]. Let 500 LESOP nodes be randomly deployed in a 50×50 square region. The network simulation time duration is set to be 120 s, and the target appears in the surveillance square at the time $t = 30$ s, and disappears at the time $t = 90$ s. Without loss of generality, we further simulate the target mobility as follows: The target velocity is fixed at 10 m/s, and the direction is a random variable uniformly distributed in $[0, 2\pi)$. The mobility direction is independently updated every 0.5 s, while the generator guarantees that the target would not move out of the surveillance region in the next time period of 0.5 s. Unless indicated, all the parameters values conform to the list in Table I. The network simulation results take the average of 100 Monte Carlo runs.

The network energy consumption of four different configurations of N and ρ are plotted in Fig. 6. In Fig. 6, it is easy to identify the time period from 30 s to 90 s, when the target is present. The network power consumption takes a much higher value in the period because P_{track} is generally much higher than P_{idle} . Fig. 7 summarizes the network energy consumption at

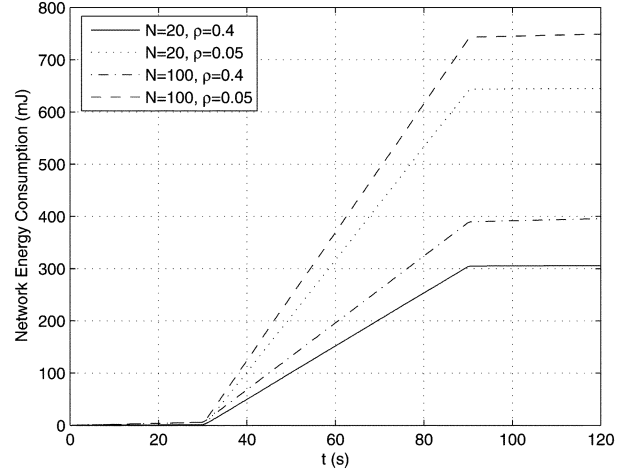
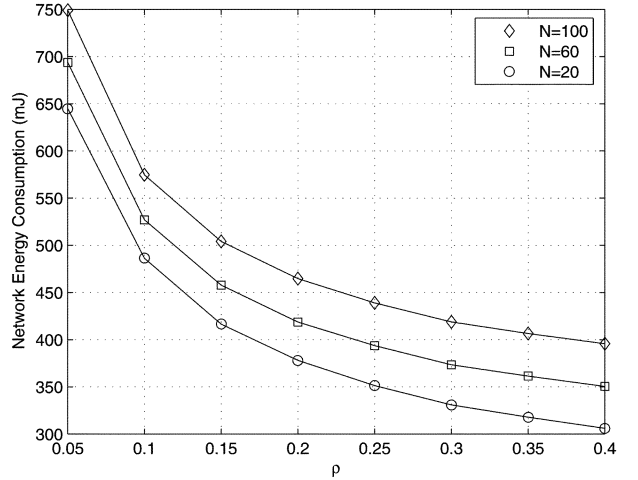


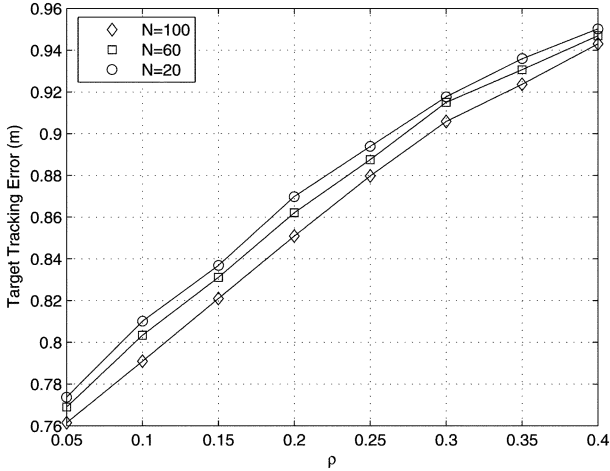
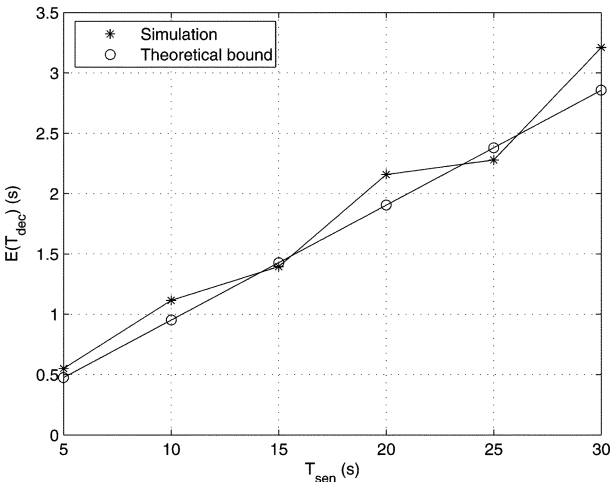
Fig. 6. Network energy consumption increasing with simulation time.

Fig. 7. Network energy consumption at $t = 120$ s versus ρ .

$t = 120$ s. Both Figs. 6 and 7 show (clearer in Fig. 7) that the network energy consumption increases with N and decreases with ρ , which confirms our previous analysis. In Fig. 7, for a given ρ , the energy consumption is observed to be linearly increasing with N , which is due to the third term of P_{track} in (35). For a fixed N , the variation of network energy consumption over ρ takes a similar curve as $N_t^*(\rho)$ (Fig. 5), which is due to the second term of P_{track} (35).

Target tracking error is defined as the average target localization error in the simulation time period. Fig. 8 shows the tracking error for different configurations of N and ρ . Similar to the previous results in Fig. 4, the tracking error generally increases with N , and decreases with ρ . Close examination also reveals that the curve of $N = 60$ and $N = 100$ are closer to each other, because the measurement error on $E_i(t)$ is inversely proportional to N (7). This error is reduced by 3 times from $N = 20$ to $N = 60$, while it is only $5/3$ times from $N = 60$ to $N = 100$.

Finally, Fig. 9 shows the variation of the expected detection delay $E(T_{\text{dec}})$ when T_{sen} changes. The parameters N and ρ are fixed at 20 and 0.2, respectively. It is observed in Fig. 9 that $E(T_{\text{dec}})$ increases linearly with T_{sen} . We observe that the simulation results and the theoretical bound (27) are close. Moreover, it is interesting to see that the simulation results are higher than the theoretical upper bound in most cases. This may be due to the boundary effect of square region, which is not taken into

Fig. 8. Target tracking error versus ρ .Fig. 9. Target detection delay $E(T_{dec})$ versus T_{sen} .

considerations in the derivation of the bound. It also indicates the tightness of the derived bound in (27).¹

VII. EMBEDDED WIRELESS INTERCONNECT

A. From OSI to EWI

Up to here, we are still using the notations inherited from classical OSI layers, such as Application, MAC, and Physical layers. However, it is easy to realize that LESOP does not even conform to the paradigm of OSI. We propose and advocate the Embedded Wireless Interconnect architecture platform, for replacing the OSI paradigm, in wireless sensor networks. The EWI is composed of two layers, which are the System layer and the Wireless Link layer, respectively. *The bottom Wireless Link layer supplies the library of wireless transmission modules to the upper System layer. The System layer judiciously decides the organization of the wireless links by exploiting the tradeoff between application-specific QoS gain and energy consumption expenditure.*

¹The LESOP sensor networks OMNet++ simulator is shared at <http://www.comm.utoronto.ca/~songl/download/LESOP/sim.zip>

Instead of consolidating OSI layers, we deem EWI as revolutionary to the OSI paradigm. The reasons are the two-fold fundamental differences between wireless sensor networks and traditional computer networks. First, data communications in sensor or pervasive computing networks are event-centric, location-centric, and data-centric. Packets routing is thus necessarily application specific. Such properties are not found in traditional computer networks, such as Internet, where the OSI paradigm is applied. Second, wireless networks, in general, have been treated as virtual wired networks in past engineering practices, by setting up virtual wired link between two mobile stations within one-hop radio distance. Significant improvements on efficiency can be achieved, by exploiting the broadcasting nature of wireless medium in wireless link modules. Such efforts, such as cooperative radio transmissions, are ideal for wireless sensor networks, where sensor nodes are deployed for one common interest.

The proposal of EWI is motivated by two trends in wireless sensor networks cross-layer design. More specifically, System layer is motivated by the first trend, which starts from the Application layer, and lets the application-specific QoS requirements define the constraints of lower layers design and optimization. The question there is, given the coding and radio communication modules, what is the optimal way to organize various aspects of the network in accomplishing application tasks, so that the network lifetime is maximized. These aspects include, but are not limited to, in-network distributed signal processing, network topology control, routing, flow/congestion control, and security/cost management. Besides LESOP, such examples can also be found in [3], [16], [24], [34], and [36]. On the other hand, Wireless Link layer is motivated by the second trend, which is focused on radio/coding modules. The question there is, given the network communication traffic pattern, what is the optimal strategy of delivering the packets so as to maximize the energy efficiency. The research necessarily leads to a compound Data Link layer and Physical layer, for which examples can be found in [30]–[33].

Moreover, a recent theoretical background study [35] also demonstrated that the separate dealing of source coding and channel coding in System layer and Wireless Linker layer, respectively, can achieve the optimal distortion and energy consumption tradeoff in reach-far wireless sensor networks, asymptotically.

The absence of a classical Network layer in EWI will not limit but rather will enhance the scalability to large-scale wireless sensor networks. The classical Network layer practice, on which diverse routing protocols rely, makes the assumption that every node is aware of its network neighborhood. However, this assumption may not hold in large-scale sensor networks, where the “neighborhood” might consist of hundreds of sensor nodes. Moreover, these sensor nodes may fall into sleep, or suffer from failures frequently over time. This suggests that the classical paradigm of network routing might not accommodate the requirements of large-scale sensor and pervasive computing networks, because of the failure of the scalability assumption. On the other hand, the suggested EWI is not constrained by this assumption to coordinate node cooperation at both the application message exchanges level and the physical data communications level, as it is clearly demonstrated by the proposed LESOP.

B. LESOP: An EWI Example

We show that LESOP virtually agrees ideally with the EWI architecture platform. In LESOP, the Application layer corresponds to the System layer under EWI. The combination of the MAC layer and the Physical layer would be the Wireless Link layer under EWI. Note that in the MAC, there is an application specific delay $T_d(\mu_i)$. Under the new EWI architecture platform, the calculation of $T_d(\mu_i)$ should be shifted to the System layer. The System layer further attaches an application specific time delay parameter to every packet forwarded to the Wireless Link layer. This parameter is $T_d(\mu_i)$ for DEC_INFO packets, while it is zero for TRACK_INFO and TRACK_ACK packets. The System layer also interacts with the Wireless Link layer by two sets of messages, which are RADIO_ACT/RADIO_SLE, and DEC_READY/DEC_CANCEL, respectively. The functions of the two sets of messages remain the same. Thus, in LESOP, we are able to identify the clear definitions of the System, and Wireless Link layers, and also the interface between the two. LESOP ideally fits in the EWI architecture platform without any further modifications.

Furthermore, in sensor networks practice, System layer needs to be at least divided into two parallel sub-layers. The first sub-layer deals with in-network signal processing for high level event acquisition, e.g., LESOP and [34]. The second sub-layer deals with the sink event query/subscription and delivery [3], [30], [36]. It is worthwhile to note that in [36], the similar interaction between the Application (System) layer and the MAC/Physical (Wireless Link) layer is utilized, as in LESOP, i.e., the application specific time delay parameter.

Although the generality of EWI is still in the pre-mature stage, it is under active investigation. In our vision, the EWI future directions can be grouped into the following two categories.

- By studying energy efficient ways of wireless link communications under different conditions, the objective is set for developing a standard wireless link modules library for System layer engineers. The abstracted category of wireless links can be broadcast [32], peer-to-peer unicast [31], to-sink unicast [30], [33], or multicast/anycast in an area. The associated module parameters need to include latency, rate, outage probability, range, and energy consumption.
- By investigating efficient network architectures of different applications, the objective is set for defining the unified interface syntax between System layer and Wireless Link layer. The objective here is also to develop efficient collaborative signal processing algorithms in distributed networks. This provides the set of design methodologies for System designers. For example, the design of LESOP also suggests a state centric programming [38] strategy in the event acquisition sub-layer of the System layer.

In general, the described delay $T_d(\mu_i)$ in LESOP, defined in the interface syntax between the System layer and the Wireless Link layer, is an application specific parameter which decides the packet scheduling in the broadcast wireless link module.

VIII. DISCUSSIONS

A. Radio Range and Sensing Range

In the LESOP design, it is assumed that the radio range, *Range*, is two times larger than the sensing range. The as-

sumption keeps the nodes set $\{i|E_i(t) > E_{th,i}\}$, i.e., target detection nodes, within the *Range* of each other. It also keeps the set within the *Range* of H_1 , i.e., $\{i|E_i(t) > E_{th,i}\} = \mathbf{A}_s$, provided the velocity constraint in Section VIII-B.

Note that sensing range is not explicitly given in the model definition. It is decided by a group of parameters, i.e., P_{FA} , σ_i^2 , γ_i , and the source signal $s(t)$. The radio range, *Range*, on the other hand, is not necessarily the single hop distance, and is determined by the specific Wireless Link layer implementation. Although multi-hop radio communications are traditionally well understood in the OSI Network layer, nevertheless, it can be implemented in Physical layer as well [32]. If single hop radio distance is smaller than sensing range, such Physical layer firing proposals are ideal for LESOP, because there would be no packet level delay incurred in consecutive hops. Then, Physical (Wireless Link) layer firing is automatically confined within the local activated region.

B. Target Moving Velocity

Let v_{\max} denote the maximum target velocity. The constraint on v_{\max} is that $v_{\max} \cdot T_{\text{track}} \leq (\text{Range}/2)$.

Provided that the radio range, *Range*, is two times larger than the sensing range, the constraint ensures that the nodes set $\{i|E_i(t) > E_{th,i}\}$ falls in the *Range* of H_1 . However, if the constraint is not satisfied, the following two conditions can take place. First, if $(\text{Range}/2) < v_{\max} \cdot T_{\text{track}} \leq ((3 \cdot \text{Range})/2)$, the tracking error can be amplified, because an incomplete set of nodes is utilized in information fusion. Second, if $v_{\max} \cdot T_{\text{track}} > ((3 \cdot \text{Range})/2)$, the target can be missed during the tracking process. Another event record will be generated when the target is detected again by sensor nodes elsewhere.

In real world implementation, the parameter T_{track} can be adaptively updated, according to the current estimation of target velocity.

C. Multiple Targets Tracking

Although most research efforts have been focused on single target tracking, multiple targets tracking also has been receiving a lot of interests. Generally, if multiple targets can be differentiated in time or space, then single target tracking protocol can work efficiently. If the condition is not satisfied, Li *et al.* [37] proposed the implementation of target classification algorithms on individual sensor nodes.

In the paper, we have only discussed single target tracking. We suggest that the multiple targets tracking problem can be solved in a similar way as [37], provided that multiple orthogonal radio channels are available, e.g., by TDMA or FDMA. When co-located multiple targets are present, the tracking of different targets can then operate on different channels concurrently, provided that the sensor nodes can classify the intrusion targets. Particularly, by modifying the LESOP implementation, the node H_1 needs to probe for a vacant channel, and broadcast the target characteristics in that particular channel, after having sent the \mathbf{B}_a beacon.

D. Coexistence Issues

As previously stated in Section VII, the System layer in sensor networks need be at least of two sub-layers, which deal with the high level event acquisition and the delivery, respectively. For target tracking sensor networks, specifically, the target tracking sub-layer, such as in LESOP, needs to

operate concurrently with the other sub-layer, i.e., the intrusion event query/delivery. Orthogonal channels (or separate radios) can enable the coexistence of the two parallel sub-layers. If half-duplex radio and real-time delivery are employed or required, System layer designers might need also to decide the associated priority between the particular two sub-layers for radio occupation.

IX. CONCLUSION

We have proposed LESOP for target tracking in wireless sensor networks, based on a holistic cross-layer design perspective. Linear processing is employed for target location estimation. Compared with the optimal nonlinear estimation, the proposed linear processing achieves significantly lower complexity, which makes it suitable for sensor networks implementation. A QoS knob coefficient ρ is found in optimizing the fundamental tradeoff. Moreover, the protocol is fully scalable because the fusion coefficient $\{\mu_i\}$ (in (19)) is calculated locally on individual sensor nodes. Additionally, the tradeoff between the detection time-delay T_{dec} and the network idle power consumption P_{idle} is found in (29) and (31), where the parameter T_{sen} is utilized to control this tradeoff.

In the protocol design of LESOP, direct interactions between the top Application layer and the bottom MAC/Physical layers were exploited. The traditional Network layer and Transport layer have been removed, thus simplifying the protocol stack. Some traditional functionalities of the two layers are merged into the top and the bottom layers. Embedded Wireless Interconnect is then proposed as the potential universal architecture for sensor networks design. Although the generality of EWI needs further investigation and definition, LESOP is shown as an example that fits ideally the EWI description. As such, it sheds light on the paradigm migration from OSI to EWI.

APPENDIX

UPPER BOUND ON $E(T_{dec})$

We divide the continuous time into small intervals δt , when target is present in the surveillance region. As long as δt is small, $E_s(t)$ and $\mathbf{L}_T(t)$ are constant within the period δt , which is $E_s(t) = E_s$ and $\mathbf{L}_T(t) = \mathbf{L}_T$. Moreover, since the conditional target detection probability on E_s within δt , $P_{dec}(\delta t|E_s)$, is also small, it can be approximated as the summation of all the detection probabilities of individual sensor nodes i , denoted by $P_{dec,i}(\delta t|E_s)$.

For an arbitrary sensor node i , there is

$$\begin{aligned}
 P_{dec,i}(\delta t|E_s) & \stackrel{(a)}{=} \text{Prob}(E_i(t) > E_{th,i}) \cdot \frac{\delta t}{T_{sen}} \\
 & \stackrel{(b)}{=} Q\left(\left(E_{th,i} - \sigma_i^2 - \frac{\gamma_i \cdot E_s}{\|\mathbf{L}_i - \mathbf{L}_T\|^2}\right) \cdot \sqrt{\frac{N}{2\max(\sigma_i^4)}}\right) \cdot \frac{\delta t}{T_{sen}} \\
 & \stackrel{(c)}{\geq} Q\left(Q^{-1}(P_{FA}) - \frac{\min(\gamma_i) \cdot E_s}{\|\mathbf{L}_i - \mathbf{L}_T\|^2} \cdot \sqrt{\frac{N}{2\max(\sigma_i^4)}}\right) \cdot \frac{\delta t}{T_{sen}} \\
 & \stackrel{(d)}{=} p(\|\mathbf{L}_i - \mathbf{L}_T\|^2) \cdot \frac{\delta t}{T_{sen}} \quad (39)
 \end{aligned}$$

where (a) is obvious, (b) is obtained from (3) and (7), (c) is due to (8), and (d) is obtained by the definition

$$p(x) = Q\left(Q^{-1}(P_{FA}) - \frac{\min(\gamma_i) \cdot E_s}{x} \cdot \sqrt{\frac{N}{2\max(\sigma_i^4)}}\right). \quad (40)$$

Due to the Poisson deploying model, (1), there is

$$\begin{aligned}
 P_{dec}(\delta t|E_s) & = \sum_i P_{dec,i}(\delta t|E_s) \\
 & \geq \frac{\delta t}{T_{sen}} \cdot \int_0^{+\infty} p(x^2) \cdot 2\pi x \lambda dx \\
 & = \frac{\pi \cdot \delta t}{T_{sen}} \cdot \lambda \cdot \int_0^{+\infty} p(x) dx. \quad (41)
 \end{aligned}$$

Thus, due to the normal distribution model of E_s , (6), the unconditional probability, $P_{dec}(\delta t)$, is

$$\begin{aligned}
 P_{dec}(\delta t) & = \int_{-\infty}^{+\infty} P_{dec}(\delta t|x) \cdot \frac{1}{\sqrt{2\pi\sigma_s^2}} \cdot e^{-\frac{(x-E_s)^2}{2\sigma_s^2}} dx \\
 & \geq \frac{\delta t}{T_{sen}} \cdot \lambda \cdot \delta p \quad (42)
 \end{aligned}$$

where δp is defined in (28). Further, given a time period Δt , there is

$$\begin{aligned}
 \text{Prob}(T_{dec} < \Delta t) & \stackrel{(a)}{=} 1 - (1 - P_{dec}(\delta t))^{\frac{\Delta t}{\delta t}} \\
 & \stackrel{(b)}{\geq} 1 - \left(1 - \frac{\delta t}{T_{sen}} \cdot \lambda \cdot \delta p\right)^{\frac{\Delta t}{\delta t}} \\
 & \stackrel{(c)}{\geq} 1 - e^{-\frac{\Delta t \cdot \lambda \cdot \delta p}{T_{sen}}} \quad (43)
 \end{aligned}$$

where (a) is due to the independence of all the small time period δt in Δt , (b) is obtained directly from (42), and (c) is a mathematical law, which holds for all $(\Delta t/T_{sen}) \cdot \lambda \cdot \delta p < 1$.

Define ϑ be an exponential random variable [25] with the mean, $E(\vartheta) = T_{sen}/(\lambda \cdot \delta p)$. The CDF of ϑ is

$$\text{Prob}(\vartheta < \Delta t) = 1 - e^{-\frac{\Delta t \cdot \lambda \cdot \delta p}{T_{sen}}}. \quad (44)$$

By combining (43) and (44), there is straightforwardly

$$E(T_{dec}) \leq E(\vartheta) = \frac{T_{sen}}{\lambda \cdot \delta p}. \quad (45)$$

REFERENCES

- [1] I. F. Akyildiz, W. Su, Y. Sankasubramaniam, and E. Cayirci, "A survey on sensor networks," *IEEE Commun. Mag.*, pp. 102–114, Aug. 2002.
- [2] S. Keshav, *An Engineering Approach to Computer Networking: ATM Networks, the Internet, and the Telephone Network*. Reading, MA: Addison-Wesley, 1997.
- [3] T. He, J. A. Stankovic, C. Lu, and T. Abdelzaher, "Speed: A stateless protocol for real-time communication in sensor networks," in *Proc. Int. Conf. Distributed Computing Systems (ICDCS)*, 2003, pp. 46–55.
- [4] DARPA Connectionless Networking Solicitation. [Online]. Available: <http://www.darpa.mil/ato/solicit/CN/>
- [5] V. Kawadia and P. R. Kumar, "A cautionary perspective on cross layer design," *IEEE Wireless Commun. Mag.*, vol. 12, no. 1, pp. 3–11, Feb. 2005.
- [6] *IEEE Trans. Acoust., Speech, Signal Process., Special Issue on Time-Delay Estimations*, vol. ASSP-29, no. 3, Jun. 1981.
- [7] S. Haykin, *Array Signal Processing*. Englewood-Cliffs, NJ: Prentice-Hall, 1985.
- [8] X. Sheng and Y. Hu, "Maximum likelihood multiple-source localization using acoustic energy measurements with wireless sensor networks," *IEEE Trans. Signal Process.* vol. 53, no. 1, pp. 44–53, Jan. 2005.

- [9] L. Doherty, K. S. J. Pister, and L. E. Ghaoui, "Convex position estimation in wireless sensor networks," in *Proc. IEEE INFOCOM*, 2001, pp. 1655–1663.
- [10] Y. Zou and K. Chakrabarty, "Target localization based on energy considerations in distributed sensor networks," in *Proc. 1st IEEE Workshop on Sensor Network Protocols and Applications (SNPA 2003)*, May 2003, pp. 51–58.
- [11] F. Zhao, J. Shin, and J. Reich, "Information-driven dynamic sensor collaboration," *IEEE Signal Process. Mag.*, vol. 19, no. 2, pp. 61–72, Mar. 2002.
- [12] M. Chu, H. Haussecker, and F. Zhao, "Scalable information-driven sensor querying and routing for ad hoc heterogeneous sensor networks," *Int. J. High Perform. Comput. Appl.*, vol. 16, no. 3, pp. 293–313, 2002.
- [13] D. Guo and X. Wang, "Dynamic sensor collaboration via sequential Monte Carlo," *IEEE J. Sel. Areas Commun.*, vol. 22, no. 6, pp. 1037–1047, Aug. 2004.
- [14] R. Brooks, P. Ramanathan, and A. Sayeed, "Distributed target classification and tracking in sensor networks," *Proc. IEEE*, vol. 91, no. 8, pp. 1163–1171, Aug. 2003.
- [15] J. Moore, T. Keiser, R. Brooks, S. Phoha, D. Friedlander, J. Koch, A. Reggio, and N. Jacobson, "Tracking targets with self-organizing distributed ground sensors," in *Proc. IEEE Aerospace Conf.*, 2003, pp. 5_2113–5_2123.
- [16] W. Zhang and G. Cao, "Optimizing tree reconfiguration for mobile target tracking in sensor networks," in *Proc. IEEE INFOCOM*, 2004, pp. 2434–2445.
- [17] H. Gupta, S. Das, and Q. Gu, "Connected sensor cover: Self-organization of sensor networks for efficient query execution," in *Proc. MobiHoc*, 2003, pp. 189–200.
- [18] X. Wang, G. Xing, Y. Zhang, C. Liu, R. Pless, and C. Gill, "Integrated coverage and connectivity configuration in wireless sensor networks," in *Proc. ACM 1st Int. Conf. Embedded Networked Sensor Systems (SenSys)*, Los Angeles, CA, 2003, pp. 28–39.
- [19] G. Gui and P. Mohapatra, "Power conservation and quality of surveillance in target tracking sensor networks," in *Proc. ACM MobiCom*, 2004, pp. 129–143.
- [20] S. Singh and C. S. Raghavendra, "PAMAS: Power aware multi-access protocol with signaling for ad hoc networks," *ACM Comput. Commun. Rev.*, vol. 28, no. 3, pp. 5–26, Jul. 1998.
- [21] W. Ye, J. Heidemann, and D. Estrin, "An energy-efficient MAC protocol for wireless sensor networks," in *Proc. IEEE INFOCOM*, 2002, pp. 1567–1576.
- [22] T. Dam and K. Langendoen, "An adaptive energy-efficient MAC protocol for wireless sensor networks," in *Proc. ACM 1st Int. Conf. Embedded Networked Sensor Systems (SenSys'03)*, Nov. 2003, pp. 171–180.
- [23] K. Jamieson, H. Balakrishnan, and Y. C. Tay, "Sift: A MAC protocol for event-driven wireless sensor networks," Massachusetts Inst. Technol., Tech. Rep. MIT-LCS-TR-894, 2003.
- [24] W. B. Heinzelman and A. P. Chandrakasan, "An application-specific protocol architecture for wireless microsensor networks," *IEEE Trans. Wireless Commun.*, vol. 1, no. 4, pp. 660–670, Oct. 2002.
- [25] A. Papoulis and S. U. Pillai, *Probability, Random Variable and Stochastic Processes*, 4th ed. New York: McGraw-Hill, 2002.
- [26] C. Guo, L. C. Zhong, and J. M. Rabaey, "Low power distributed MAC for ad hoc sensor radio networks," in *Proc. IEEE GLOBECOM*, 2001, pp. 2944–2948.
- [27] C. Shurgers, V. Tsiatsis, S. Ganeriwal, and M. Srivastava, "Optimizing sensor networks in the energy-latency-density design space," *IEEE Trans. Mobile Comput.*, vol. 1, no. 1, pp. 70–80, Jan.–Mar. 2002.
- [28] A. Varga, "OMNeT++: Discrete Event Simulation System User Manual," [Online]. Available: <http://www.omnetpp.org/external/doc/html/usman.php>
- [29] J. G. Proakis, *Digital Communication*, 3rd ed. New York: McGraw-Hill, 1995.
- [30] L. Song and D. Hatzinakos, "Architecture of sensor networks with mobile sinks: Sparsely deployed sensors," *IEEE Trans. Veh. Technol.*, Jul. 2007, to be published.
- [31] L. Song and D. Hatzinakos, "Cooperative transmission in Poisson distributed wireless sensor networks: protocol and outage probability," *IEEE Trans. Wireless Commun.*, vol. 5, no. 10, pp. 2834–2843, Oct. 2006.
- [32] A. Scaglione and Y. W. Hong, "Opportunistic large arrays: Cooperative transmission in wireless multihop ad hoc networks to reach far distances," *IEEE Trans. Signal Process.*, vol. 51, no. 8, pp. 2082–2092, Aug. 2003.
- [33] P. Venkitasubramaniam, S. Adireddy, and L. Tong, "Opportunistic ALOHA and cross-layer design for sensor networks," in *Proc. IEEE Military Commun. Conf.*, Oct. 2003, pp. 705–710.
- [34] C. Guestrin, P. Bodik, R. Thibaux, M. Paskin, and S. Madden, "Distributed regression: An efficient framework for modeling sensor network data," in *Proc. 3rd Int. Symp. Information Processing in Sensor Networks (IPSN 2004)*, Apr. 2004, pp. 1–10.
- [35] L. Song and D. Hatzinakos, "Energy efficiency limits of broadcasting in wireless networks," *IEEE Trans. Wireless Communications*, May 2005, submitted for publication.
- [36] O. Goussevskaia, M. Machado, R. Mini, A. Loureiro, G. Mateus, and J. Nogueira, "Data dissemination based on the energy map," *IEEE Commun. Mag.*, vol. 43, no. 7, pp. 134–143, Jul. 2005.
- [37] D. Li, K. Wong, Y. Hu, and A. Sayeed, "Detection, classification, and tracking of targets," *IEEE Signal Process. Mag.*, vol. 19, no. 2, pp. 17–29, Mar. 2002.
- [38] J. Liu, M. Chu, J. Liu, J. Reich, and F. Zhao, "State-centric programming for sensor-actuator network systems," *IEEE Pervasive Comput.*, vol. 2, no. 4, pp. 50–62, Oct.–Dec. 2003.



Liang Song (S'03–M'06) received the Bachelor degree in electrical engineering from Shanghai Jiaotong University, China, in 1999, the M.S. degree in electronic engineering from Fudan University, China, in 2002, and the Ph.D. degree from the Edward S. Rogers Sr. Department of Electrical and Computer Engineering, University of Toronto, Canada, in 2005.

His research and development experience include the areas of wireless communications and networking, signal processing, and information theory. The application areas include telecommunications service providing, low power mesh networking for emergent interconnections, wireless sensor networks for intelligent surveillance and biomedical signal acquisition. His publications include the authoring of over twenty research papers in technical journals and conference proceedings, while he is also the leading inventor of two patent pending innovations in the area of wireless communications and networking. His industrial experience includes the consulting through SENNET Communications and CANAMET Inc.



Dimitrios Hatzinakos (M'90–SM'98) received the Diploma degree from the University of Thessaloniki, Greece, in 1983, the M.A.Sc degree from the University of Ottawa, Canada, in 1986, and the Ph.D. degree from Northeastern University, Boston, MA, in 1990, all in electrical engineering.

In September 1990, he joined the Department of Electrical and Computer Engineering, University of Toronto, where now he holds the rank of Professor with tenure. Also, he served as Chair of the Communications Group of the Department from July 1999 to June 2004. Since November 2004, he has been the holder of the Bell Canada Chair in Multimedia at the University of Toronto. His research interests are in the areas of multimedia signal processing and communications. He is an author or co-author of more than 150 papers in technical journals and conference proceedings, and he has contributed to eight books in his areas of interest. His experience includes consulting through Electrical Engineering Associates Ltd. and contracts with United Signals and Systems Inc., Burns and Fry Ltd., Pipetronix Ltd., Defense Research Establishment Ottawa (DREO), Nortel Networks, Vivosonic Inc. and CANAMET Inc.

Prof. Hatzinakos served as an Associate Editor for the IEEE TRANSACTIONS ON SIGNAL PROCESSING from 1998 to 2002, and Guest Editor for the special issue of *Signal Processing* on Signal Processing Technologies for Short Burst Wireless Communications, which appeared in October 2000. He was a member of the IEEE Statistical Signal and Array Processing Technical Committee (SSAP) from 1992 to 1995 and Technical Program co-Chair of the 5th Workshop on Higher-Order Statistics in July 1997. He is a member of EURASIP, the Professional Engineers of Ontario (PEO), and the Technical Chamber of Greece.